Journal of the Geological Society

Duration of the Early Bajocian and the associated $\delta^{13}C$ positive excursion based on cyclostratigraphy

Baptiste Sucheras-Marx, Fabienne Giraud, Vincent Fernandez, Bernard Pittet, Christophe Lecuyer, Davide Olivero and Emanuela Mattioli

Journal of the Geological Society 2013, v.170; p107-118.
doi: 10.1144/jgs2011-133

Notes

Journal of the Geological Society, London, Vol. **170**, 2013, pp. 107–118. doi: 10.1144/jgs2011-133.

Duration of the Early Bajocian and the associated $\delta^{13}C$ positive excursion based on cyclostratigraphy

BAPTISTE SUCHERAS-MARX[1*], FABIENNE GIRAUD[2], VINCENT FERNANDEZ[3], BERNARD PITTET[1], CHRISTOPHE LECUYER[1], DAVIDE OLIVERO[1] & EMANUELA MATTIOLI[1]

[1]*UMR CNRS 5276 LGL-TPE, Université Claude Bernard Lyon 1, Ecole Normale Supérieure Lyon, Campus de la DOUA, Bâtiment Géode, 69622 Villeurbanne cedex, France*

[2]*ISTerre, UMR 5275, Université Joseph Fourier Grenoble, 1381 rue de la piscine, BP 53, 38041 Grenoble cedex 9, France*

[3]*Bernard Price Institute for Palaeontological Research, University of the Witwatersrand, Private Bag 3, Johannesburg 2050, South Africa*

**Corresponding author (e-mail: baptiste.sucheras@gmail.com)*

Abstract: The Early Bajocian, about 172 Ma ago, was a period of tectonic changes, a global carbon-isotope positive excursion, and biological diversification of marine invertebrates (e.g. ammonites, radiolarians and coccolithophores). Unfortunately, both the duration of the Early Bajocian and the associated palaeoenvironmental changes are still poorly constrained. We propose here an estimate of the duration of this sub-stage based on a cyclostratigraphic analysis of the carbonate content from the Chaudon–Norante section, French Subalpine Basin, France. The Chaudon–Norante succession has been correlated with Les Dourbes section using greyscale variations to detect possible local hiatuses. The duration estimated here for the entire Early Bajocian is 4.082 Ma. Two intervals were identified in the positive $\delta^{13}C$ excursion: an increase of carbon isotope values lasting 1.36 Ma and climax isotope values lasting for 2.72 Ma. A cooling at high latitudes and warming at low latitudes may have enhanced the Earth's temperature gradient leading to an increase in humidity, which in turn triggered ocean eutrophication at the origin of the $\delta^{13}C$ positive excursion.

Supplementary material: The complete dataset presented in the paper, a colour version of the figure 8 and correlation of $\delta^{13}C$ excursions between our studied site and contemporaneous sites are available at www.geolsoc.org.uk/SUP18555.

During the Early Bajocian (*c.* 172 Ma; Middle Jurassic), a $\delta^{13}C$ positive excursion with global impact is recorded in the carbonate sediments and it is concomitant with the diversification of various oceanic groups such as coccolithophores (Cobianchi *et al*. 1992; Mattioli & Erba 1999; Bown *et al*. 2004), radiolarians (Bartolini *et al*. 1996) and ammonites (O'Dogherty *et al*. 2006). This carbon isotope excursion (CIE) has been identified in several places in Europe (Corbin 1994; Bartolini *et al*. 1996, 1999; Jenkyns *et al*. 2002; O'Dogherty *et al*. 2006; Brigaud *et al*. 2009), and is characterized by an amplitude of +1‰ recorded in bulk carbonates (well documented by O'Dogherty *et al*. 2006) and +2‰ in belemnites (e.g. Jenkyns *et al*. 2002). However, the positive CIE is not well observed in coal and organic matter deposits from Yorkshire (Hesselbo *et al*. 2003). It is therefore unclear if the excursion affected all the carbon reservoirs. This perturbation is explained as being the result of an increase in primary productivity owing to ocean fertilization (Bartolini *et al*. 1999). Despite the major perturbations affecting both the biosphere and geosphere as recorded in sedimentary rocks of that age, no accurate time frame has been offered for the collective end-Aalenian–Early Bajocian period. As radiochronology for this time interval is still highly uncertain (Pálfy *et al*. 2000; Hall *et al*. 2004), the current duration of 2 Ma proposed for the Early Bajocian was based on the supposition that the ammonite subzones were of equal duration, each lasting 200 ka in the Bajocian (Gradstein *et al*. 2004).

Since the recognition of cyclic deposition in the sedimentary record from the calcium carbonate content related to orbital cycles (Gilbert 1895), the cyclostratigraphic method has been widely used to constrain durations of several Mesozoic stages (e.g. Claps *et al*. 1995; Giraud *et al*. 1995; Boulila *et al*. 2008; Suan *et al*. 2008*b*; Huang *et al*. 2010). Based on cyclostratigraphic analysis of calcium carbonate content obtained from hemipelagic deposits of the Chaudon–Norante section (France), we present here a new estimate of the duration of the Early Bajocian. Moreover, the new $\delta^{13}C_{carb}$ data presented here allow a good identification of the carbon cycle perturbation and an estimation of its duration.

Geological and palaeogeographical settings

Two sections were studied for this work: Chaudon–Norante and Les Dourbes. Both of these sections are located in the French Subalpine Basin, which was delimited northward by the Jura platform, westward by the Central Massif and the Ardèche platform, and southward by the Provence platform (Fig. 1a). These two sections belong to the Digne tectonic Nappe (Southern Alps), emplaced during the Mio-Pliocene (Lemoine 1973; Gidon & Pairis 1992). Chaudon–Norante was used here as a reference for the calculation of the Early Bajocian duration. A comparison was made with the hemipelagic Les Dourbes succession, the thickest section for the Early Bajocian interval from the French Subalpine Basin, to highlight possible hiatuses in the sedimentary succession in Chaudon–Norante. Les Dourbes section was also used to retrieve the long-term sedimentation rate.

Chaudon–Norante

The Chaudon–Norante section, located in the Ravin de Coueste near Digne (Fig. 1b), presents a continuous succession from the

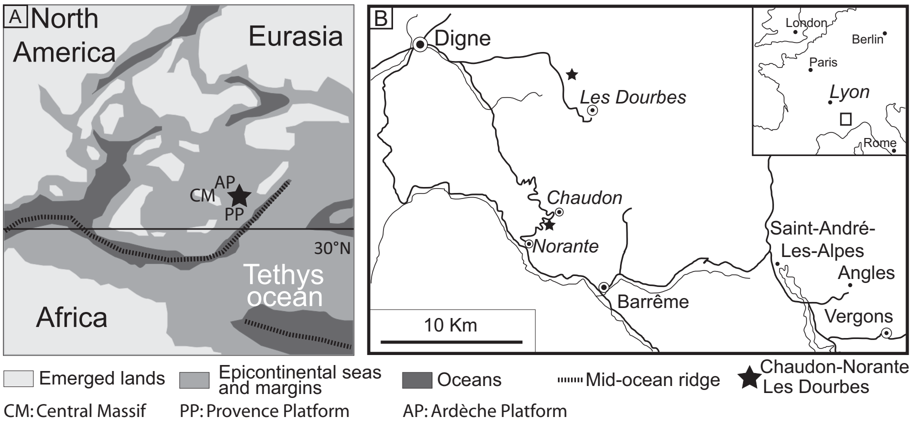

Fig. 1. (**a**) Geographical location of Les Dourbes and Chaudon–Norante in France. (**b**) Palaeogeography of Europe during the Middle Jurassic, modified from Scotese (2001) and Blakey (2005). The map shows the distribution of the emerged lands, epicontinental seas, deep oceans and mid-ocean ridges. The black star represents the location of Les Dourbes and Chaudon–Norante in the French Subalpine basin.

Toarcian (Early Jurassic) to the base of the Bathonian (Middle Jurassic). This section was proposed for the Aalenian–Bajocian GSSP (Erba & Pavia 1990). The Chaudon–Norante succession is well exposed and the ammonite biostratigraphy for the Bajocian (Pavia 1973, 1983) as well as the nannofossil biostratigraphy have high temporal resolution (Erba 1990; Mattioli & Erba 1999).

The part of the section studied here extends from the end of the Aalenian to the end of the Early Bajocian (Fig. 2). The succession comprises decimetre-scale hemipelagic marlstone–limestone alternations. The limestones are mainly wackestones to packstones with some bioclastic remains of *Bositra* (Bivalvia), radiolarians, rare benthic foraminifera and rare siliceous sponge spicules (Pavia 1983).

The latest Aalenian is assigned to the latest part of the Concavum ammonite Zone. This 39.6 m thick interval is composed of fairly regular marlstone–limestone alternations except for the uppermost part, which is marl-dominated. The 129 m thick Early Bajocian succession corresponds to four ammonite zones. The Discites Zone at the base is dominated by marlstone. The Laeviuscula Zone displays regular marlstone–limestone alternations. The Sauzei Zone is limestone-dominated, whereas the Humphriesianum Zone displays regular marlstone–limestone alternations (Fig. 2).

Les Dourbes

Les Dourbes section is located in the Ravin de Feston, near Digne (Fig. 1b). This section generally presents the same sedimentary succession as in the Chaudon–Norante section. It is characterized by metre-scale hemipelagic limestone–marlstone alternations over 235 m for the Early Bajocian (Fig. 3). At Les Dourbes, a high-resolution ammonite zonation was proposed only for the part ranging from the boundary between the Sauzei and Humphriesianum Zones, to the Early Bajocian–Late Bajocian boundary (Pavia 1983). The biochronology of the lower part of the section (Discites and Laeviuscula Zones) is derived from Ferry & Mangold (1995) but without any precise identification of the zone limits.

Analytical methods

Analysis of calcium carbonate content and of sediment greyscale

For the calcium carbonate content, the Chaudon–Norante section has been regularly sampled every 15 cm, which has provided 251 samples for the latest Aalenian and 873 samples for the whole Early Bajocian. Each of the 1124 samples has been analysed using a Dietrich–Frühling calcimeter to determine the wt% $CaCO_3$ contents by measuring the CO_2 evolved after acidification of the sample.

We compared the low-frequency greyscale representations to correlate precisely the two sections, which are also correlated by means of ammonite biostratigraphy, and thus detect possible hiatuses in the thinner Chaudon–Norante section. Owing to the abundant vegetation present on both sections, and the difficulty of overcoming the problem of shadows altering the greyscale intensity in pictures, we performed the greyscale representation on precise drawings of the sections with bed by bed measurements. The Chaudon–Norante section was previously described (Pavia 1983) with great accuracy, including a precise thickness measurement of each bed and the associated lithology. Four lithological groups were recognized (i.e. marlstone, calcareous marlstone, argillaceous limestone and limestone) and each of them was associated with a grey level on an 8 bits greyscale (256 grey levels). Hence we obtained a general greyscale representation of the section with zero for marlstone, 85 for calcareous marlstone, 170 for argillaceous limestone and 255 for limestone, showing grey-level alternations in agreement with field observations of carbonate content. Les Dourbes section was previously studied (Ferry & Mangold 1995) following the method described by Pavia (1983), so a similar greyscale representation was obtained for this section using our protocol.

Based on these artificial greyscale representations of the sections, we extracted the grey value of each pixel along each section to obtain scatter plots (greyscale/thickness of the section). We obtained 2371 values for the Chaudon–Norante section and 4319 values for Les Dourbes. As the aim of these greyscale representations was to correlate the sections we applied a smoothing filter to each plot to retrieve the low-frequency (long-term) signal of the sedimentary deposits. The smoothing has been performed using a moving average calculation padded with the last values on 150 points for Les Dourbes and 75 points for Chaudon–Norante using the Stratigraphic Analysis Software Strati-Signal 1.0.5 (Ndiaye 2007). The smoothing process leads to loss in value number (n) owing to averaging. The padding method is a mathematical method that fills the value loss by interpolation.

Stable carbon isotope ratios of bulk carbonates

Carbon isotope compositions of bulk samples have been measured using a Multiprep auto-sampler coupled to a GV Isoprime® mass spectrometer. For this bulk carbon isotope analysis, we selected 101 samples from the whole sample set, all having a $CaCO_3$ content ≥80 wt% to limit possible problems owing to differential diagenesis in marlstones and limestones. For each sample, an aliquot of 300–375 µg of rock proportional to the $CaCO_3$ concentration was reacted with anhydrous oversaturated phosphoric acid at 90 °C for 20 min. Isotopic compositions are quoted in the delta notation in

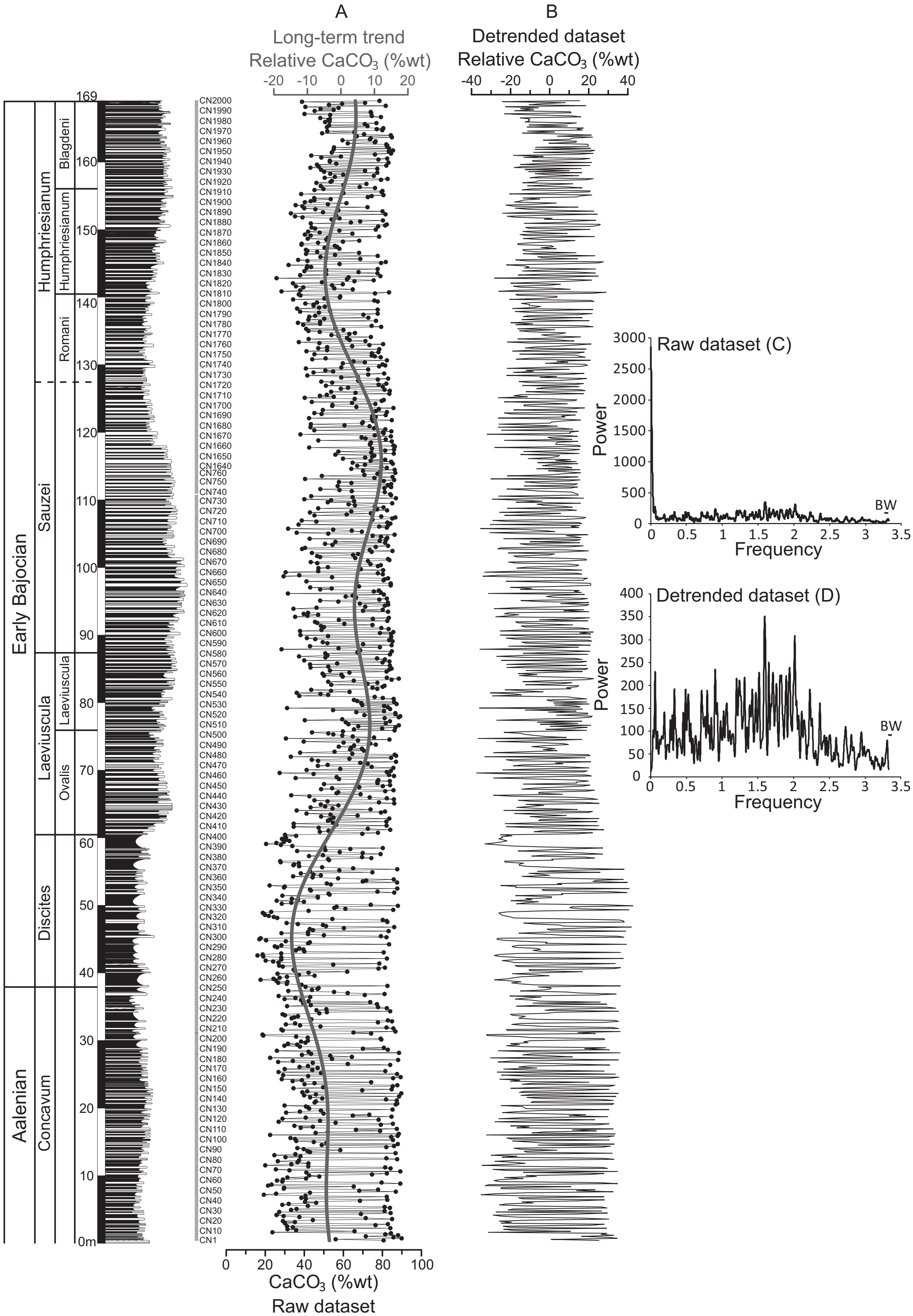

Fig. 2. The Chaudon–Norante section modified from Pavia (1983). (**a**) The raw dataset. The Blackman-Tuckey (BT) analysis 'raw dataset' (**c**) is strongly influenced by a long-term frequency. This frequency extracted, which has a period of 77 m ± 39 m, is represented in grey (**a**) as well as the residuals obtained, called the detrended dataset (**b**), and represented by relative $CaCO_3$. The BT analysis 'detrended dataset' (**d**) shows the main frequencies observed on the residuals dataset without the influence of the long-term variations. The bandwidth (BW) for spectral analyses is 0.03.

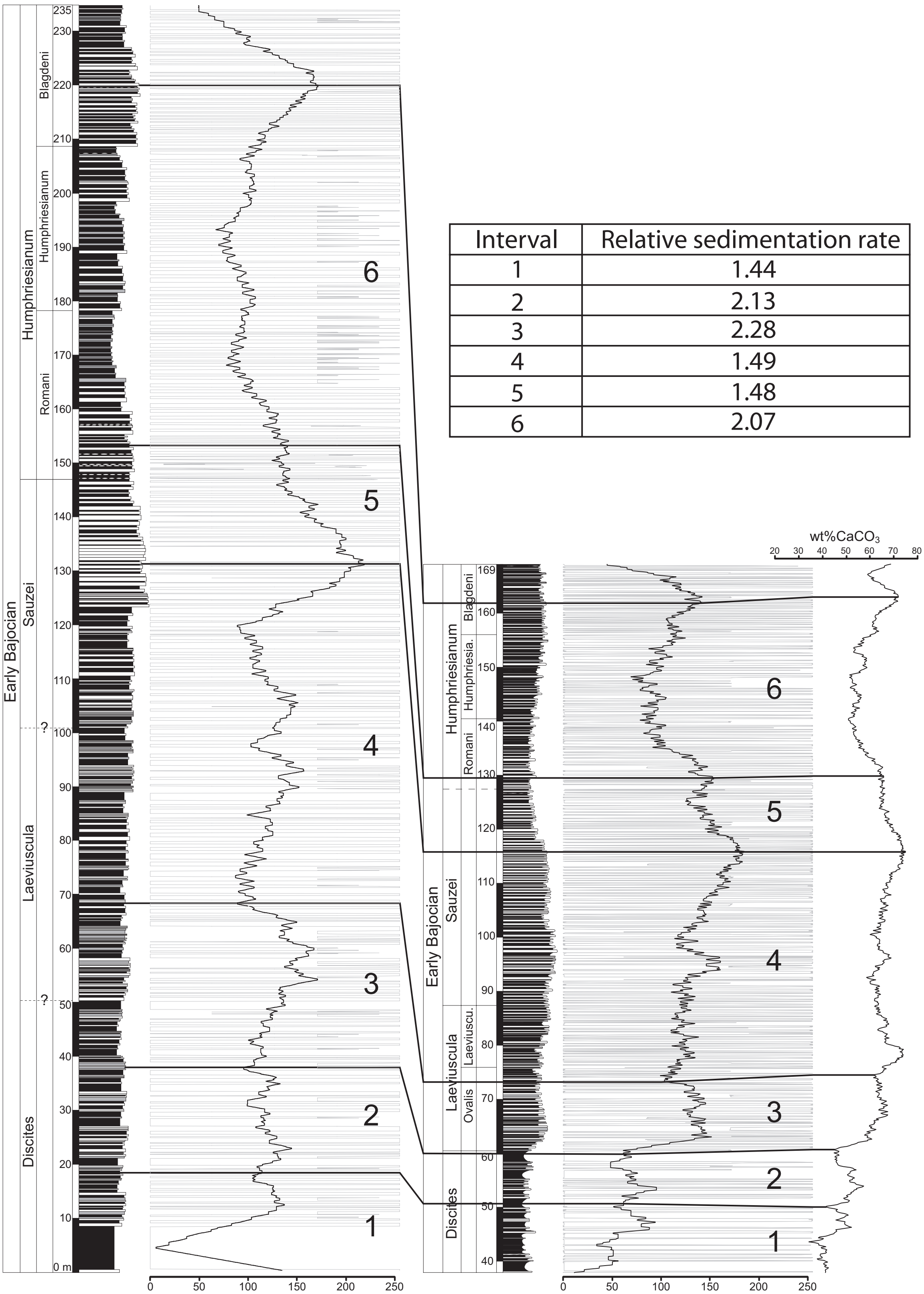

Interval	Relative sedimentation rate
1	1.44
2	2.13
3	2.28
4	1.49
5	1.48
6	2.07

Fig. 3. Grey-level representations on 8 bit greyscales of Les Dourbes sections (left; based on Pavia 1983 and Ferry & Mangold 1995) and of the Chaudon–Norante section (right; based on Pavia 1983). Both results have been smoothed using a moving average with padding method from StratiSignal with a 150 point interval for Les Dourbes and a 75 point interval for Chaudon–Norante. Re-sampled $CaCO_3$ content is also represented smoothed with a 25 point interval. Good correlations with the grey-level graphs are observed. Based on the greyscale correlations, six intervals are proposed with relative sedimentation rate between Les Dourbes and Chaudon–Norante reported in the table.

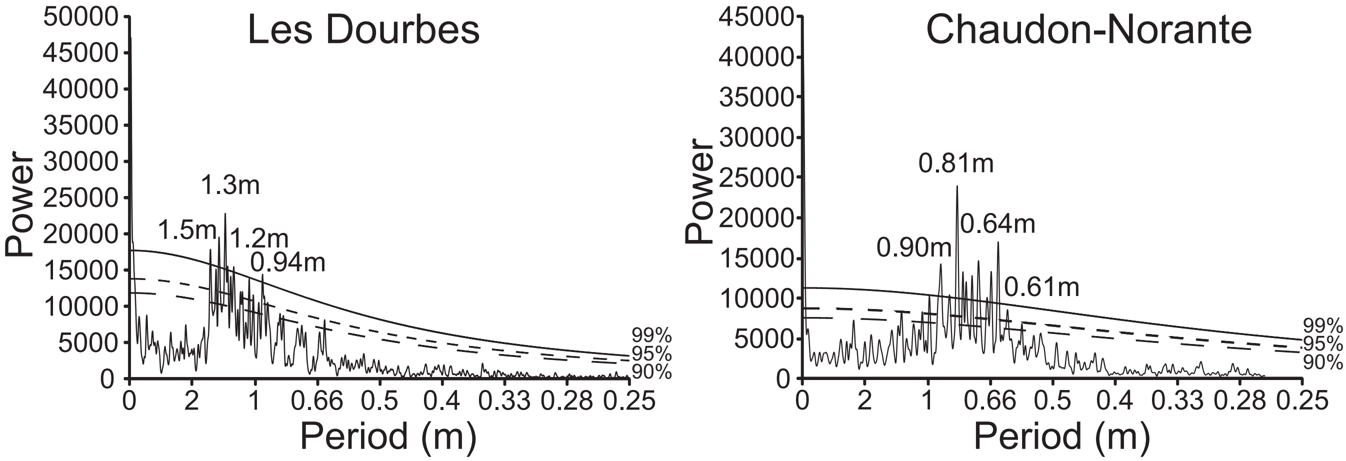

Fig. 4. Two spectral analyses based on greyscale extracted from Les Dourbes (left) and Chaudon–Norante (right). The confidence levels have been calculated using the method of Mann & Lees (1996). At Les Dourbes, periods ranging from 1.5 to 0.94 m are supported with confidence interval over 99%. At Chaudon–Norante, periods ranging from 0.9 to 0.64 m are supported with confidence interval over 99%. These periods from both sections represent the limestone–marlstone alternations.

permil relative to VPDB. All sample measurements were duplicated and adjusted to the international reference NIST NBS19. External reproducibility was on average *c*. 0.05‰ (2σ) for $\delta^{13}C_{carb}$ values.

Spectral analysis techniques

Various spectral analysis methods have been used although the algorithms employed for each technique are not discussed in this study. We refer to Weedon (2003) for the basic mathematics and to Paillard *et al*. (1996) for algorithms for spectral analyses performed using AnalySeries (Paillard *et al*. 1996).

The Blackman–Tuckey (BT) method was first used on the grey values extracted for Chaudon–Norante and Les Dourbes (Figs 3 and 4), and for the Chaudon–Norante wt% $CaCO_3$ time series (Fig. 2a). The lowest frequency spectral peak of the wt% $CaCO_3$ time series from Chaudon–Norante, representing a 77 ± 39 m long-term trend, has been band-pass filtered using AnalySeries (Fig. 2a). The resulting new time series represented in relative $CaCO_3$ (wt%; Fig. 2b) has been analysed using the BT method with a Bartlett window and 0.03 and 0.08 m long bandwidths (Fig. 5b and c). Confidence levels were determined by the robust method of Mann & Lees (1996), determining the red-noise function by a least-squares approach using the software R 2.12.0 (R Development Core Team, Vienna, Austria). On the same time series, a Multi-Taper Method (MTM) with six tapers was also used with the lower and upper error bars (Fig. 5a). Finally, a Morlet wavelet analysis (Torrence & Compo 1998) was also performed to highlight possible variations in short-term sedimentary wavelengths. This analysis is presented with frequencies $\omega_0 = 6$ and $\omega_0 = 24$.

Results

Greyscale spectral analysis and correlation between Les Dourbes and Chaudon–Norante

At Les Dourbes, the grey levels fluctuate between 100 and 170 until the middle of the Sauzei Zone, where the grey level increases to 220 to the end of the Sauzei Zone. The Humphriesianum Zone displays low greyscale values before an increase at the end of this zone. At Chaudon–Norante, the grey levels are low, between 50 and 100, in the Discites Zone. Grey level increases to 180 in Laeviuscula Zone and reaches 180 at the end of the Sauzei Zone. The Humphriesianum Zone displays low grey-level values before an increase at the end of this zone.

The variations in the carbonate content deduced from grey-level variations at Les Dourbes (235 m thick) and Chaudon–Norante (131 m thick) sections show very similar stratigraphic trends (Fig. 3). Thus, the thickness ratio between comparable intervals of the two successions is the relative sedimentation rate. The ratio of relative sedimentation rate for the Early Bajocian between these two sections is 1.79, which corresponds to the ratio of thickness (in metres) for the whole Early Bajocian between the two studied sections. We recognized six intervals on the basis of their grey-level correlations and calculated the relative sedimentation rate for each of them. From the base to the top of the Early Bajocian, the relative sedimentation rates for each interval are respectively 1.44, 2.13, 2.28, 1.49, 1.48 and 2.07. The correlations based on ammonite zones cannot be used straightforwardly to establish the relative sedimentation rate in these two sections, because at Les Dourbes only the upper part of the section (i.e. Humphriesianum Zone and the upper part of the Sauzei Zone) was precisely dated by ammonites (Pavia 1983). No hiatuses were identified at Chaudon–Norante or Les Dourbes by using the grey-level correlation technique, but only variable accumulation rates.

Both spectral analyses on the grey-level variations reveal two main groups of frequency supported by confidence intervals over 99% (Fig. 4). The ranges of these groups of peak periods are linked to variations in sedimentation rate. In both sections, these peaks represent the limestone–marlstone alternations. The ratio of mean frequencies over 99% observed between Les Dourbes and Chaudon–Norante is *c*. 1.6 (Fig. 4). Thus, this ratio of carbonate alternations is close to the relative sedimentation rate estimated above based on the correlations. This observation allows us to consider the difference of thickness in limestone–marlstone alternation in both sections as the result of a variable sedimentation rate rather than the presence of hiatuses in the Chaudon–Norante deposits (Fig. 3).

Calcium carbonate content at Chaudon–Norante

At the base of the section, in the Concavum and Discites Zones, the range of the $CaCO_3$ content is wider than in the rest of the section (Fig. 2). Fluctuations between 20 and 85 wt% are observed. In the Concavum Zone, $CaCO_3$ mostly ranges from 30 to 85 wt%. Within the large-scale variations, there is a rise between 10 and 20 m with

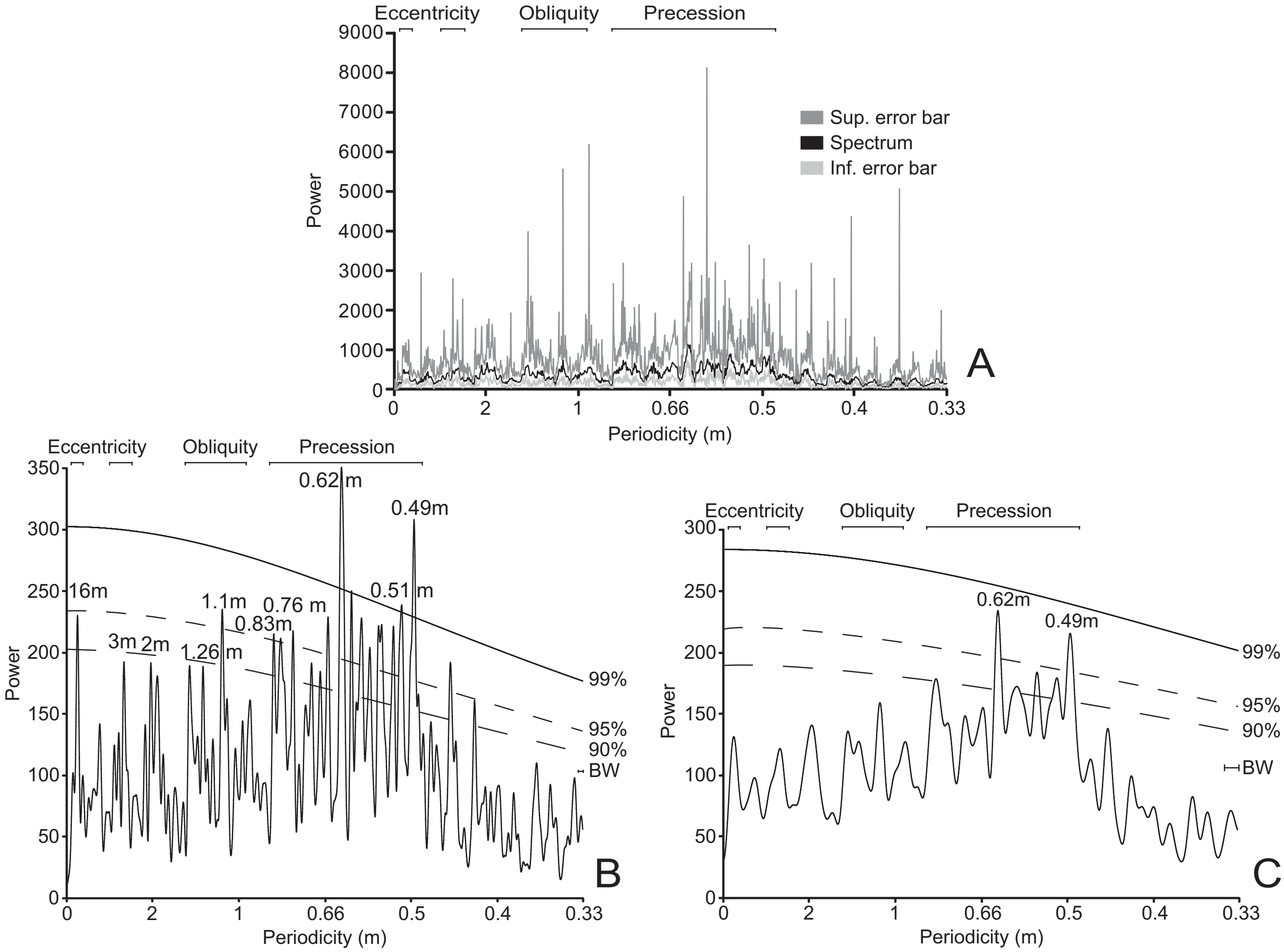

Fig. 5. Spectral analyses of wt% $CaCO_3$ from Chaudon–Norante. (**a**) Multi-taper analysis. (**b**, **c**) Two Blackman–Tuckey (BT) analyses, with a bandwidth (BW) of 0.03 (**b**) and 0.08 (**c**). The confidence intervals have been calculated on BT analyses based on the method of Mann & Lees (1996). Based on the hierarchical organization of the periods observed, ranges for the eccentricity, obliquity and precession cycles are presented.

a slight reduction of the range of the small-scale fluctuations of the $CaCO_3$ contents. Then, there is a decrease in the large-scale variations of $CaCO_3$ content from 20 to 40 m. In the Laeviuscula Zone, the range of $CaCO_3$ content decreases and varies between 40 and 85 wt%. In the Sauzei Zone, the range of $CaCO_3$ content decreases even more and varies locally between 50 and 85 wt%. This decrease is linked to a long-scale overall rise in the $CaCO_3$ content. Finally, in the Humphriesianum Zone, the $CaCO_3$ range is 40 wt% wide. In this zone, there is a decrease of the $CaCO_3$ content from 128 to 142 m, followed by an increase from 142 to 165 m. The long-scale variations are less prominent after the extraction of the long-period cycle observed through the spectral analysis (see Material and Methods) but this filtering does not affect the small-scale $CaCO_3$ variations and ranges in different intervals.

Carbon isotope curve of Chaudon–Norante

The $\delta^{13}C_{carb}$ plot can be divided into three parts (Fig. 6). The first part, ranging from the base of the section to the Aalenian–Bajocian boundary, has $\delta^{13}C$ values fluctuating between 1 and 1.5‰ with three values below 1‰ but without any clear long-term pattern. The second part, from the Aalenian–Bajocian boundary to the end of the Laeviuscula ammonite Zone, shows a progressive increase from 1.3 to 2.5‰. The third part, from the end of the Laeviuscula ammonite Zone to the end of the Early Bajocian, displays steady values fluctuating between 2.3 and 2.7‰ with three points below 2.2‰. In this part, there is a weak trend towards a reduction of 0.3‰.

$CaCO_3$ spectral analysis at Chaudon–Norante

Based on the results from the MTM and BT spectral analyses, different groups of spectral peaks are recognized (Fig. 5). On the 0.3 m bandwidth BT analysis, the cycles with a period of 16, 1.1, 0.83, 0.76 and 0.52 m are supported with a confidence level over 95%. The 0.62, 0.51 and 0.49 m cycles are supported with a confidence level over 99%. The 0.62 and 0.49 m cycles are again supported on the 0.8 m bandwidth BT analysis over 95%. All the main frequencies obtained with the BT method are also obtained with the MTM method (Fig. 5). The 0.62 and 0.49 m cycles correspond to the marlstone–limestone alternations observed in the field and on the greyscale spectral analysis.

We propose to interpret the different groups of peaks based on the hierarchical organization of the Milankovitch cycles (i.e. eccentricity 405 ka and *c.* 100 ka, obliquity 41 ka, and precession 23 ka and 19 ka), which can be summarized from precession to eccentricity as 1:2:5:20. In prior geological times, the duration of obliquity

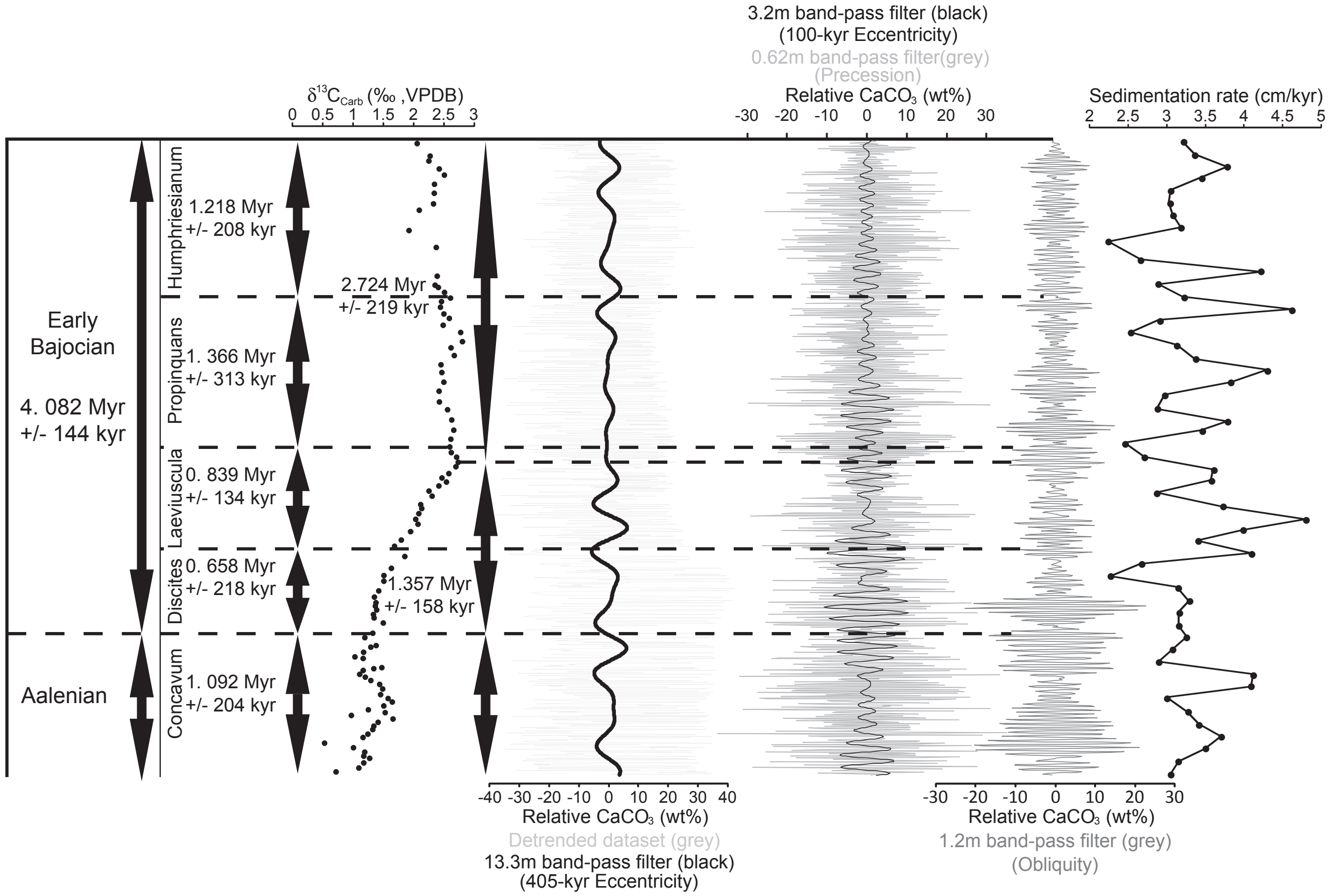

Fig. 6. Filtered Milankovitch cycles from the $CaCO_3$ at Chaudon–Norante. The $CaCO_3$ detrended dataset (grey) is represented with the 13.3 m (width from 20–10 m) band-pass filter (black; 405 ka eccentricity) on the left, the 3.2 m (width from 3.85–2.78 m) band-pass filter (black; 100 ka eccentricity) and the 0.62 m (width from 0.84–0.48 m) band-pass filter (grey; precession) cycles in the middle, the 1.2 m (width from 1.43–0.98 m) band-pass filter (black; obliquity) cycle on the right. Proposed durations for the Early Bajocian, its four ammonite zones and the $\delta^{13}C_{carb}$ positive excursion are presented for each interval.

and precession was probably shorter than in the Quaternary and can be approximated (Berger & Loutre 1994), and estimations for the eccentricity behaviour for the last 250 Ma have been proposed (Laskar *et al*. 2004, 2011*a*) although the chaotic behaviour of large asteroids in the Solar System means that a precise determination of the evolution of Earth's eccentricity is not possible (Laskar *et al*. 2011*b*). Nevertheless, the hierarchical organization of orbital cycles should have been consistent through time and can still be used (Berger & Loutre 1994). The shorter cycle observed, with periods from 0.48 to 0.84 m, is attributed to precession. The second one, with period ranging from 0.98 to 1.43 m, is assigned to obliquity. The third one, with periods from 2.8 to 3.84 m, is assigned to the high-frequency eccentricity, whereas the last range of periods (12–16 m) corresponds to the low-frequency eccentricity. Unfortunately, these hypotheses about cycle identification cannot yet be supported by absolute dating from radiochronology.

Filtering, age quantification and sedimentation rate

In Figure 6 are reported the filtered variations of $CaCO_3$ wt% contents for the periods corresponding to the precession (periods from 0.84 to 0.48 m), obliquity (periods from 1.43 to 0.98 m), and 100 ka (periods from 3.84 to 2.77 m) and 405 ka eccentricity (periods from 10 to 20 m) cycles. We observe, on the basis of these filtered data, that most of the variations of $CaCO_3$ contents may be explained by the precession and obliquity cycles. The effects of the 405 ka eccentricity cycle are not as strongly recorded as in the $CaCO_3$ signal, despite the high confidence level for the associated period in the spectral analysis. Eccentricity is acknowledged to be the only orbital cycle to have most probably remained close to steady state from the Mesozoic to the Quaternary (Laskar *et al*. 2004). The 100 ka eccentricity cycle, which is not supported in the spectral analysis, is more represented during the latest Aalenian and the beginning of the Early Bajocian and then fades away in the Sauzei and Humphriesianum ammonite Zones. Moreover, the obliquity cycle, strongly represented in the latest Aalenian, seems to fade away in the upper part of the Discites ammonite Zone and the rest of the Early Bajocian. This cycle is well recorded in the $CaCO_3$ content variations at the transition between the Laeviuscula and the Sauzei ammonite Zones.

The 405 ka eccentricity cycle for the past 250 Ma is the more stable cycle in the Phanerozoic (Laskar *et al*. 2004) and has been used to quantify the duration of the stratigraphic interval studied. However, because of the poor representation of the 405 ka eccentricity cycle, the duration of the Early Bajocian, ammonite zones and the $\delta^{13}C$ excursion has also been quantified based on the 100 ka eccentricity cycle, the obliquity and the precession. The obliquity cycle is supposed to have a period of 37 ka and the precession cycle is supposed to have a period of 20 ka (Berger & Loutre 1994). The results are presented in the Table 1. We propose for each time interval a duration value (mean in the Table 1) that is the mean of

Table 1. *Sub-stages, ammonite zones and isotopic steps duration estimations based on the four filtered Milankovitch cycles*

Time interval	Duration 405 ka filtered (ka)	Duration 100 ka filtered (ka)	Duration 37 ka filtered (ka)	Duration 20 ka filtered (ka)	Mean (ka)	2σ (ka)
Sub-Stage						
Late Aalenian (part)	940	1130	1137.75	1160	1092	204
Early Bajocian	4100	4080	3986.75	4160	4082	144
Ammonite zones						
Concavum (part)	940	1130	1137.75	1160	1092	204
Discites	510	770	693.75	660	658.5	218
Laeviuscula	910	770	795.5	880	839	134
Sauzei	1600	1270	1295	1300	1366	313
Humphriesianum	1080	1270	1202.5	1320	1218	208
Isotopic steps						
Increase	1240	1410	1378.25	1400	1357	158
Plateau	2860	2670	2608.5	2760	2724.5	219

For each time interval, an average duration corresponding to the arithmetic mean of the four estimations is given with the associated error (2σ)

durations calculated from each Milankovitch cycle. We are more confident in these mean duration values than in durations calculated only from the 405 ka eccentricity cycle, which is commonly used for such time estimation but is not well defined in our succession. The standard deviation associated with a mean value is given as the error (2σ). The latest Aalenian part of the section lasted 1.092 ± 0.204 Ma but this duration is not equivalent to the entire Concavum Zone, as its lower limit was not recorded at Chaudon–Norante. The Early Bajocian lasted 4.082 ± 0.144 Ma. All durations proposed in this study and associated errors are summarized in Table 1.

The sedimentation rates have been calculated at Chaudon–Norante using a tuning method based on correlations with the modelled eccentricity cycle La2010d proposed by Laskar *et al*. (2010*a*) and our filtered 405 ka eccentricity and 100 ka eccentricity cycles. The sedimentation rate does not display a long-term trend and shows minimum and maximum values of 2 and 5 cm ka^{-1}. Most of the high sedimentation rate intervals correspond to more carbonate-rich intervals and most of the low sedimentation rate intervals correspond to less carbonate-rich intervals.

Wavelet analysis

The cycles corresponding to precession are relatively continuous in Chaudon–Norante, with a weak signal between 35 and 40 m, 75 and 85 m, and from 161 m upward to the end of the section (P in Fig. 7). The cycles corresponding to obliquity are less consistent. They are especially strongly expressed between 30 and 60 m (O in Fig. 7). The cycles corresponding to 100 ka eccentricity are inconsistently expressed, especially between 10 and 30 m and from 100 m upward to the end of the section (e in Fig. 7). Finally, the cycle corresponding to the 405 ka eccentricity is almost continuous except between 85 and 105 m, and from 135 m upward to the end of the section (E in Fig. 7).

Discussion

Sedimentation and cyclicity

No hiatuses were identified at Chaudon–Norante on the basis of field observations or greyscale correlations with the thick and continuous Les Dourbes section. Stratigraphic continuity is also supported on the basis of the correspondence of cycles observed in the two studied sections. The duration of the Early Bajocian can thus be precisely and confidently calculated at Chaudon–Norante by means of cyclostratigraphy. The Chaudon–Norante section, which presents regular marlstone–limestone couplets, has been selected for the cyclostratigraphic method rather than the GSSP Cabo Mondego in Portugal, which has more nodular limestones and less regularly alternating couplets (Suchéras-Marx *et al*. 2012). The observed sedimentary carbonate cycles can be produced by factors such as changes in productivity of pelagic carbonate (productivity cycle), in carbonate mud export from shallower areas (export cycle) or in siliciclastic input from the hinterland, or by diagenetic processes (Einsele & Ricken 1991; Einsele 1996; Pittet & Strasser 1998). Models of diagenetically induced cycles are often based on carbonate dissolution in relation to aragonite transformation (Munnecke *et al*. 2001; Westphal *et al*. 2004). These models can easily explain the limestone–marlstone alternations but cannot explain the hierarchical organization of cycles such as the one observed at Chaudon–Norante. Moreover, they fail to explain the long-distance correlation observed between Les Dourbes and Chaudon–Norante. During the Early Bajocian at Cabo Mondego, Portugal, the carbonate pelagic production by calcareous nannofossils increased but represents only 20% of the total carbonate (Suchéras-Marx *et al*. 2012). At Chaudon–Norante, the carbonate pelagic production is equal to or lower than at Cabo Mondego (Suchéras-Marx 2012). Thus, pelagic productivity cycle cannot explain the genesis of the carbonate cycles observed at Chaudon–Norante. Siliciclastic dilution cycles cannot be ruled out but, based on correlations between the Jura platform and the Digne area (i.e. Chaudon–Norante and Les Dourbes), some researchers have argued that the sedimentation in the basin during the Bajocian was essentially controlled by the export of carbonate from the platform (Ferry & Mangold 1995; Thiry-Bastien 2002).

The cycles identified by time-series analysis, as far as they have been identified in carbonate content variations, may have recorded either changes in the amount of carbonate produced on the platform itself and then delivered to the basin, or changes in the intensity of carbonate export from the platform to the basin, without necessarily important changes in the shallow-area carbonate production. Carbonate production on platforms is commonly related to climatically driven environmental conditions or to sea-level variations (Hallock & Schlager 1986; Pittet *et al*. 2000). Also, platform morphology coupled to sea-level variations can play a major role in platform export intensity. Flat-topped platforms can be subaerially exposed during low sea levels, resulting in both a decrease in carbonate production and basinward export (Schlager *et al*. 1994; Pittet *et al*. 2000). In contrast, carbonate ramp systems are less affected by changes in production rates during sea-level fluctuations (Reuning *et al*. 2002), because the shallow locus of carbonate

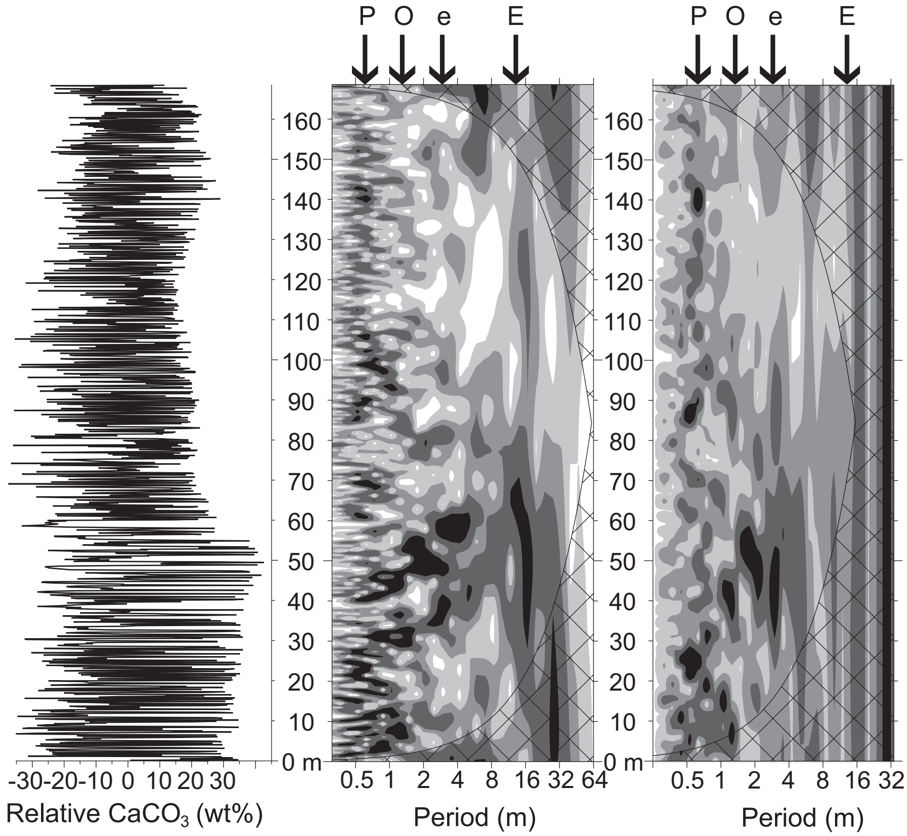

Fig. 7. Two wavelet analyses based on the method of Torrence & Compo (1998) and correlated to the relative $CaCO_3$ of the detrended dataset. The wavelet analysis on the right has been carried out using a 6 Morlet frequency and that on the left using a 24 Morlet frequency. The arrows show the periods for Milankovitch cycles identified on the spectral analyses (P, precession; O, obliquity; e, 100 ka eccentricity; E, 405 ka eccentricity).

production will move along the ramp profile, following the sea level (Gréselle & Pittet 2010). On the other hand, the export of carbonates from the shallow areas to the basin was more efficient during lowstand in platforms with ramp morphology owing to reduction of the distance from the production area to the accumulation area, as shown for the Valanginian of the Vocontian Basin (Gréselle & Pittet 2010). During the Bajocian, carbonate export dynamics from the Jura carbonate ramp to the Subalpine basin were also more efficient during lowstand of sea level as evidenced by important carbonate deposits corresponding to a lowstand systems tract in the basin (Ferry & Mangold 1995; Thiry-Bastien 2002). Hence, the carbonate content at Les Dourbes and Chaudon–Norante is probably controlled by sea-level export cycles. Such cycles produced by export of carbonate from platforms have already been documented in various Jurassic stages and carbonate-dominated sections in Europe (Pittet & Strasser 1998; Mattioli & Pittet 2002; Pittet & Mattioli 2002; Olivier *et al*. 2004; Suan *et al*. 2008*a*; Bádenas *et al*. 2009). Nevertheless, correlations between the Jura platform and the Vocontian basin have been made at the scale of the third-order cycle (*sensu* Vail *et al*. 1991), which may be related either to tectonics or to climatically driven eustatic sea-level changes. The fluctuations in carbonate content recorded in the studied section could be climatically driven by eustatic cycles but the resolution of the correlations between the Jura platform and the Chaudon–Norante section cannot by itself completely confirm a control by Milankovitch cycles of sea-level fluctuations.

Duration of the Early Bajocian and of the $\delta^{13}C$ positive excursion

We quantified the duration of the Early Bajocian at about 4.082 Ma based on the bandpass filtering of the various astronomical cycles (Table 1). This result clearly differs from the previous 2 Ma duration proposed by Gradstein *et al*. (2004), who considered an equal duration for all the ammonite subzones of the Bajocian. Cyclostratigraphy has been frequently used and validated for Jurassic (e.g. Claps *et al*. 1995; Hinnov & Park 1999; Weedon & Jenkyns 1999; Kemp *et al*. 2005; Suan *et al*. 2008*a*) and Cretaceous times (e.g. Giraud *et al*. 1995; Locklair & Sageman 2008; Huang *et al*. 2010) providing more rigorous duration estimations than those previously inferred from ammonite biochronology. Radiometric ages have been proposed in the last ammonite zone of the Aalenian and the first ammonite zone of the Late Bajocian based on Canadian deposits (Pálfy *et al*. 2000). Based on those results, the Early Bajocian is a little shorter than 7.6 Ma. Unfortunately, the errors associated with ages proposed for the Middle Jurassic are longer than the proposed duration of the stage, and no confidence linked to this duration is available so far (Pálfy *et al*. 2000; Gradstein *et al*. 2004). The proposed duration for the Early Bajocian as well as its four ammonite zones can be used as reference, as Chaudon–Norante ammonite biostratigraphy is well defined and has been used in the definition of Bajocian biochronostratigraphy (Pavia 1983; Rioult *et al*. 1997; Gradstein *et al*. 2004).

Our cyclostratigraphic estimates also allow us to discuss the duration of the positive CIE recorded in Chaudon–Norante as well as in several other European sites. The duration of a C isotope perturbation is a key parameter for the understanding of the driving mechanism(s). The Early Bajocian $\delta^{13}C$ positive excursion is very well identified and can be separated into two intervals. The first interval is marked by increasing carbon isotope ratios and lasted 1.357 Ma ± 158 ka. The second interval corresponds to climax $\delta^{13}C$ values and lasted 2.724 Ma ± 219 ka.

Other significant positive C isotope excursions are known in the geological record. The Late Cenomanian carbon isotope positive excursion, associated with the Oceanic Anoxic Event 2 (OAE2; around 94 Ma), is one of the most important and studied positive CIEs during the Mesozoic. It has been estimated as having a duration of 197 ka (increase values *c*. 90 ka and climax *c*. 107 ka, Kuhnt *et al*. 2005), 430 ka (Voigt *et al*. 2008) or 572–601 ka (Sageman *et al*. 2006). Although there is debate about the estimation of the duration of the OAE2, this event was shorter than 1 Ma and thus shorter than the Early Bajocian carbon isotope positive excursion. The OAE2 is contemporaneous with a rapid warming of surface and shallow waters (Huber *et al*. 1999), a rapidly rising sea level (Voigt *et al*. 2006) and an increased rate of organic carbon burial at the origin of the positive CIE. Despite some similarities between the Late Cenomanian and the Early Bajocian, anoxia in the oceans, the worldwide organic-rich deposits and the duration of the OAE2 event challenge its comparison with the Early Bajocian event. The Weissert Event (Erba *et al*. 2004), a carbon isotope positive excursion occurring during the Valanginian (*c*. 136 Ma), has been estimated to last *c*. 2 Ma (Erba 2004), 2.3 Ma (Sprovieri *et al*. 2006) or 1.5 Ma until the interval where $\delta^{13}C$ values start decreasing (Gréselle & Pittet 2010; Gréselle *et al*. 2011). This major positive CIE is interpreted as an increase in primary production (Stoll & Schrag 2000; Erba & Tremolada 2004) in relation to more humid conditions in enhanced greenhouse conditions possibly triggered by the Paraña–Etendeka volcanic province activity (Erba *et al*. 2004; Weissert & Erba 2004). Thus, the Early Bajocian carbon isotope positive excursion has a duration of the same order of magnitude as the Weissert Event and may have related origins.

The Early Bajocian is also an time of great changes in marine biota. The most important one is a large diversification of ammonoids with a major turnover corresponding to the disappearance of the Hildoceratoidae and the diversification of the Stephanoceratoidae and the Hammatoceratoidae (Pavia 1983; Cresta 1988; Rioult *et al*. 1997). There is a major change in coccolithophores with the diversification of the genus *Watznaueria*, whose species have dominated the nannofossil assemblage for 80 Ma (Erba 2006). Although this is beyond the scope of the present study, the new time scale for the Early Bajocian presented here will help the quantification of evolutionary rates and lead to a better understanding of diversification rate in marine biota.

Climatic conditions in the Early Bajocian

During the Early Bajocian, a temperature increase of the Tethys Ocean has been observed based on oyster and belemnite $\delta^{18}O$ (Dera *et al*. 2011). On the other hand, large glendonites, indicators of cool conditions, were deposited in Siberia during the Bajocian, although these occurrences lack precise correlation with European biostratigraphic schemes (Price 1999; Rogov & Zakharov 2010). Hence, if both warming at low latitudes and cooling at high latitudes are synchronous, a progressive increase in latitudinal temperature gradient during the beginning of the Early Bajocian had occurred.

The positive $\delta^{13}C$ excursion has been linked to an increase in primary production related to a diversification and increase of coccolith abundance under eutrophic conditions (Suchéras-Marx *et al*. 2012). Such a process could have resulted from increasing flux of continentally derived nutrients (Bartolini *et al*. 1996; O'Dogherty *et al*. 2006) or increasing intensity or frequency of monsoon or storm activity (Price *et al*. 1998) as already proposed for the genesis of Hungarian deposits (Raucsik *et al*. 2001; Raucsik & Varga 2008). The increase in the latitudinal temperature gradient would have enhanced the atmospheric mass flux from the equator to the poles, and with it the rainfall, explaining the increase in weathering and/or in storm activity (Price *et al*. 1998). Thus, the $\delta^{13}C$ positive excursion could be the consequence of a significant climate change. The origin of this climate change remains hypothetical but might be linked to an increase in volcanic activity that was documented at the Aalenian–Bajocian boundary (Bartolini & Larson 2001). This scenario is close to the one proposed for the Late Valanginian carbon isotope positive excursion (Weissert Event) (described by Gréselle *et al*. 2011 and Barbarin *et al*. 2012; see references therein), a better documented geological event than the Early Bajocian positive CIE. In addition to the climatic, geochemical and biological similarities between the Early Bajocian and the Late Valanginian, these two geological events also have similar durations. Further comparison would lead to a better understanding of the climatic and geological mechanisms driving these carbon cycle perturbations.

Conclusion

For the first time, a duration for the Early Bajocian (Middle Jurassic) has been estimated by means of a cyclostratigraphy study applied to the calcium carbonate content of sediments in Chaudon–Norante, France. According to previous studies (Pavia 1983; Ferry & Mangold 1995; Thiry-Bastien 2002) and greyscale-based correlations with Les Dourbes section, no hiatuses or sedimentary condensed intervals have been identified, providing confidence in the duration scheme we propose, as follows: (1) the Early Bajocian lasted *c*. 4.082 Ma; (2) the Discites zone lasted 0.66 Ma, the Laeviuscula zone 0.84 Ma, the Sauzei (synonym of Propinquans as recorded in other areas) 1.37 Ma, and the Humphriesianum zone 1.22 Ma; (3) the Early Bajocian $\delta^{13}C$ positive excursion has been separated into two intervals, the first characterized by increasing values and lasting 1.36 Ma, and the second by high steady-state values for 2.72 Ma.

A drastic climate change is observed during the Early Bajocian that was at the origin of the $\delta^{13}C$ positive excursion through the initiation of more humid climatic conditions and of an oceanic fertilization.

We are grateful to the Réserve Naturelle Géologique de Haute Provence and M. Guiomar for their help in the organization of the field work. H. Saffrey, J.-P. Duyé, P. Lazarin, L. Leroy, D. Bert, C. Raffin and P. Paillat are thanked for their help in sampling. M. Boussaha greatly helped in the carbonate content analysis. F. Martineau performed the stable isotope analysis of bulk carbonates. G. Suan's remarks greatly improved an earlier version of this paper. We warmly thank reviewers S. Hesselbo and S. Batenburg and the editor J. Hendry for constructive reviews of this paper. This paper is a part of B.S.-M.'s PhD project funded by the French Ministry of Research and supported by BQR UCBL Lyon1 2006 to F.G., BQR UCBL Lyon1 2010 and INSU 2011-12 Syster/Interrvie to E.M. This paper is a contribution of the team Paléoenvironnements to the UMR CNRS 5276.

References

Bádenas, B., Aurell, M., García-Ramos, J.C., González, B. & Piñuela, L. 2009. Sedimentary vs. diagenetic control on rhythmic calcareous successions (Pliensbachian of Asturias, Spain). *Terra Nova*, **21**, 162–170.

Barbarin, N., Bonin, A., *et al*. 2012. Evidence for a complex Valanginian nannoconid decline in the Vocontian basin (South East France). *Marine Micropaleontology*, **84–85**, 37–53.

Bartolini, A. & Larson, R.L. 2001. Pacific microplate and the Pangea supercontinent in the Early to Middle Jurassic. *Geology*, **29**, 735–738.

Bartolini, A., Baumgartner, P.O. & Hunziker, J.C. 1996. Middle and Late Jurassic carbon stable-isotope stratigraphy and radiolarite sedimentation of the Umbria–Marche Basin (Central Italy). *Eclogae Geologicae Helvetiae*, **89**, 811–844.

Bartolini, A., Baumgartner, P.O. & Guex, J. 1999. Middle and Late Jurassic radiolarian palaeoecology versus carbon-isotope stratigraphy. *Palaeogeography, Palaeoclimatology, Palaeoecology*, **145**, 43–60.

Berger, A.L. & Loutre, M.F. 1994. Astronomical forcing through geological time. *In*: De Boer, P.L. & Smith, D.G. (eds) *Orbital Forcing and Cyclic Sequences*. International Association of Sedimentologists, Special Publications, **19**, 15–24.

Blakey, R. 2005. Global paleogeography. World Wide Web Address: http://jan.ucc.nau.edu/~rcb7/globaltext2.html.

Boulila, S., Hinnov, L.A., *et al.* 2008. Astronomical calibration of the Early Oxfordian (Vocontian and Paris basins, France): Consequences of revising the Late Jurassic time scale. *Earth and Planetary Science Letters*, **276**, 40–51.

Bown, P.R., Lees, J.A. & Young, J.R. 2004. Calcareous nannoplankton evolution and diversity through time. *In*: Thierstein, H.R. & Young, J.R. (eds) *Coccolithophores: From Molecular Processes to Global Impact*. Springer, Berlin, 481–508.

Brigaud, B., Durlet, C., Deconinck, J.-F., Vincent, B., Pucéat, E., Thierry, J. & Trouiller, A. 2009. Facies and climate/environmental changes recorded on a carbonate ramp: A sedimentological and geochemical approach on Middle Jurassic carbonates (Paris Basin, France). *Sedimentary Geology*, **222**, 181–206.

Claps, M., Erba, E., Masetti, D. & Melchiorri, F. 1995. Milankovitch-type cycles recorded in Toarcian black shales from the Belluno trough (Southern Alps, Italy). *Memoire di Scienze Geologiche*, **47**, 179–188.

Cobianchi, M., Erba, E. & Pirini-Radrizzani, C. 1992. Evolutionary trends of calcareous nannofossil genera *Lotharingius* and *Watznaueria* during the Early and Middle Jurassic. *Memoire di Scienze Geologiche*, **43**, 19–25.

Corbin, J.C. 1994. *Evolution géochimique du Jurassique du Sud-Est de la France: influence du niveau marin et de la tectonique*. PhD thesis, Université Paris VI.

Cresta, S. 1988. Associations d'ammonites et biostratigraphie de l'Aalenien et du Bajocien inférieur des Apennins d'Ombrie-Marches (Italie Centrale). *In*: Rocha, R.B. & Soares, A.F. (eds) *2nd International Symposium on Jurassic Stratigraphy, Lisboa*. Centro de Estratigrafia e Paleobiologia da Universidade Nova de Lisboa (INIC), **1**, 209–224.

Dera, G., Brigaud, B., *et al.* 2011. Climatic ups and downs in a disturbed Jurassic world. *Geology*, **39**, 215–218.

Einsele, G. 1996. Event deposits: the role of sediment supply and relative sea-level changes—overview. *Sedimentary Geology*, **104**, 11–37.

Einsele, G. & Ricken, W. 1991. Limestone–marl alternation—an overview. *In*: Einsele, G., Ricken, W. & Seilacher, A. (eds) *Cycles and Events in Stratigraphy*. Springer, Berlin, 23–47.

Erba, E. 1990. Calcareous nannofossil biostratigraphy of some Bajocian sections from the Digne area (SE France). *Memorie Descrittive della Carta Geologica d'Italia*, **XL**, 237–256.

Erba, E. 2004. Calcareous nannofossils and Mesozoic oceanic anoxic events. *Marine Micropaleontology*, **52**, 85–106.

Erba, E. 2006. The first 150 million years history of calcareous nannoplankton: Biosphere–geosphere interactions. *Palaeogeography, Palaeoclimatology, Palaeoecology*, **232**, 237–250.

Erba, E. & Pavia, G. 1990. Record of the discussion about the proposals for the Bajocian GSSP. *Memorie Descrittive della Carta Geologica d'Italia*, **XL**, 63–68.

Erba, E. & Tremolada, F. 2004. Nannofossil carbonate fluxes during the Early Cretaceous: Phytoplankton response to nutrification episodes, atmospheric CO_2, and anoxia. *Paleoceanography*, **19**, PA1008.

Erba, E., Bartolini, A. & Larson, R.L. 2004. Valanginian Weissert oceanic anoxic event. *Geology*, **32**, 149–152.

Ferry, S. & Mangold, C. 1995. Faciès de dépôt et stratigraphie séquentielle des calcaires bajociens du Jura méridional. *Documents des Laboratoires de Géologie de Lyon*, **133**, 1–96.

Gidon, M. & Pairis, J.L. 1992. Relations entre le charriage de la Nappe de Digne et la structure de son authochtone dans la vallée du Bès (Alpes-de-Haute-Provence, France). *Eclogae Geologicae Helvetiae*, **85**, 327–359.

Gilbert, G.K. 1895. Sedimentary measurement of Cretaceous time. *Journal of Geology*, **3**, 121–127.

Giraud, F., Beaufort, L. & Cotillon, P. 1995. Astronomical control of carbonate record in the Lower Cretaceous of the Vocontian basin (SE France). *Bulletin de la Société Géologique de France*, **166**, 409–421.

Gradstein, F., Ogg, J. & Smith, A. 2004. *A Geologic Time Scale*. Cambridge University Press, Cambridge.

Gréselle, B. & Pittet, B. 2010. Sea-level reconstructions from the Peri-Vocontian Zone (South-east France) point to Valanginian glacio-eustasy. *Sedimentology*, **57**, 1640–1684.

Gréselle, B., Pittet, B., *et al.* 2011. The Valanginian isotope event: A complex suite of palaeoenvironmental perturbations. *Palaeogeography, Palaeoclimatology, Palaeoecology*, **306**, 41–57.

Hall, R.L., McNicoll, V., Gröcke, D.R., Craig, J. & Johnston, K. 2004. Integrated stratigraphy of the lower and middle Fernie Formation in Alberta and British Columbia, Western Canada. *Rivista Italiana di Paleontologia e Stratigrafia*, **110**, 61–68.

Hallock, P. & Schlager, W. 1986. Nutrient excess and the demise of coral reefs and carbonate platforms. *Palaios*, **1**, 389–398.

Hesselbo, S.P., Morgans-Bell, H.S., McElwain, J.C., Rees, P.M., Robinson, S.A. & Ross, C.E. 2003. Carbon-cycle perturbation in the middle Jurassic and accompanying changes in the terrestrial paleoenvironment. *Journal of Geology*, **111**, 259–279.

Hinnov, L.A. & Park, J.J. 1999. Strategies for assessing Early–Middle (Pliensbachian–Aalenian) Jurassic cyclochronologies. *Philosophical Transactions of the Royal Society of London*, **357**, 1831–1859.

Huang, C., Hinnov, L., Fischer, A.G., Grippo, A. & Herbert, T. 2010. Astronomical tuning of the Aptian Stage from Italian reference sections. *Geology*, **38**, 899–902.

Huber, B.T., Leckie, R.M., Norris, R.D., Bralower, T.J. & Cobabe, E. 1999. Foraminiferal assemblage and stable isotopic change across the Cenomanian–Turonian boundary in the subtropical North Atlantic. *Journal of Foraminiferal Research*, **29**, 392–417.

Jenkyns, H.C., Jones, C.E., Gröcke, D.R., Hesselbo, S.P. & Parkinson, P.N. 2002. Chemostratigraphy of the Jurassic System: Applications, limitations and implications for palaeoceanography. *Journal of the Geological Society, London*, **159**, 351–378.

Kemp, D.B., Coe, A.L., Cohen, A.S. & Schwark, L. 2005. Astronomical pacing of methane release in the Early Jurassic period. *Nature*, **437**, 396–399.

Kuhnt, W., Luderer, F., Nederbragt, S., Thurow, J. & Wagner, T. 2005. Orbital-scale record of the late Cenomanian–Turonian oceanic anoxic event (OAE-2) in the Tarfaya Basin (Morocco). *International Journal of Earth Sciences*, **94**, 147–159.

Laskar, J., Robutel, P., Joutel, F., Gastineau, M., Correia, A.C.M. & Levrard, B. 2004. A long-term numerical solution for the insolation quantities of the Earth. *Astronomy and Astrophysics*, **428**, 261–286.

Laskar, J., Fienga, A., Gastineau, M. & Manche, H. 2011*a*. La2010: a new orbital solution for the long-term motion of the Earth. *Astronomy and Astrophysics*, **532**, A89.

Laskar, J., Gastineau, M., Delisle, J.-B., Farrés, A. & Fienga, A. 2011*b*. Strong chaos induced by close encounters with Ceres and Vesta. *Astronomy and Astrophysics*, **532**, L4.

Lemoine, M. 1973. About gravity gliding tectonics in the western Alps. *In*: De Jong, K.A. & Scholten, R. (eds) *Gravity and Tectonics*. Wiley, New York, 201–216.

Locklair, R.E. & Sageman, B.B. 2008. Cyclostratigraphy of the upper Cretaceous Niobrara Formation, Western Interior, U.S.A: A Coniacian–Santonian orbital timescale. *Earth and Planetary Science Letters*, **269**, 540–553.

Mann, M.E. & Lees, J.M. 1996. Robust estimations of background noise and signal detection in climatic time series. *Climate Change*, **33**, 409–445.

Mattioli, E. & Erba, E. 1999. Synthesis of calcareous nannofossil events in Tethyan Lower and Middle Jurassic successions. *Rivista Italiana di Paleontologia e Stratigrafia*, **105**, 343–376.

Mattioli, E. & Pittet, B. 2002. Contribution of calcareous nannoplankton to carbonate deposition: A new approach applied to the Lower Jurassic of central Italy. *Marine Micropaleontology*, **45**, 175–190.

Munnecke, A., Westphal, H., Elrick, M. & Reijmer, J.J.G. 2001. The mineralogical composition of precursor sediments of calcareous rhythmites: A new approach. *International Journal of Earth Sciences*, **90**, 795–812.

Ndiaye, M. 2007. A multipurpose software for stratigraphic signal analysis. PhD thesis, Université de Genève.

O'Dogherty, L., Sandoval, J., Bartolini, A., Bruchez, S., Bill, M. & Guex, J. 2006. Carbon-isotope stratigraphy and ammonite faunal turnover for the Middle Jurassic in the Southern Iberian palaeomargin. *Palaeogeography, Palaeoclimatology, Palaeoecology*, **239**, 311–333.

Olivier, N., Pittet, B. & Mattioli, E. 2004. Palaeoenvironmental control on sponge–microbialite reefs and contemporaneous deep-shelf marl–limestone deposition (Late Oxfordian, southern Germany). *Palaeogeography, Palaeoclimatology, Palaeoecology*, **212**, 233–263.

Paillard, D., Labeyrie, L. & Yiou, P. 1996. Macintosh program performs time-series analysis. *EOS Transactions, American Geophysical Union*, **77**, 379.

Pálfy, J., Mortensen, J.K., Smith, P.L., Friedman, R.M., McNicoll, V. & Villeneuve, M. 2000. New U–Pb zircon ages integrated with ammonite biochronology from the Jurassic of the Canadian Cordillera. *Canadian Journal of Earth Science*, **37**, 549–567.

Pavia, G. 1973. Ammoniti del Baiociano superiore di Digne (Francia SE, Dip. Basses-Alpes). *Bollettino della Societa Paleontologica Italiana*, **19**, 75–142.

Pavia, G. 1983. *Ammoniti e biostratigrafia del Baiociano inferiore di Digne (Francia SE, Dip. Alpes-Haute-Provence)*. Monografie Museo Regionale di Scienze Naturali (Torino), **254**.

Pittet, B. & Mattioli, E. 2002. The carbonate signal and calcareous nannofossil distribution in an Upper Jurassic section (Balingen–Tieringen, Late Oxfordian, southern Germany). *Palaeogeography, Palaeoclimatology, Palaeoecology*, **179**, 71–96.

Pittet, B. & Strasser, A. 1998. Depositional sequences in deep-shelf environments formed through carbonate-mud import from the shallow platform (Late Oxfordian, German Swabian Alb and eastern Swiss Jura). *Eclogae Geologica Helvetica*, **91**, 149–169.

Pittet, B., Strasser, A. & Mattioli, E. 2000. Depositional sequences in deep-shelf environments: a response to sea-level changes and shallow-platform carbonate productivity (Oxfordian, Germany and Spain). *Journal of Sedimentary Research*, **70**, 392–407.

Price, G.D. 1999. The evidence and implications of polar ice during the Mesozoic. *Earth-Science Reviews*, **48**, 183–210.

Price, G.D., Valdes, P.J. & Sellwood, B.W. 1998. A comparison of GCM simulated Cretaceous 'greenhouse' and 'icehouse' climates: implications for the sedimentary record. *Palaeogeography, Palaeoclimatology, Palaeoecology*, **142**, 123–138.

Raucsik, B. & Varga, A. 2008. Climato-environmental controls on clay mineralogy of the Hettangian–Bajocian successions of the Mecsek Mountains, Hungary: An evidence for extreme continental weathering during the early Toarcian oceanic anoxic event. *Palaeogeography, Palaeoclimatology, Palaeoecology*, **265**, 1–13.

Raucsik, B., Demény, A., Borbély-Kiss, I. & Szabó, G. 2001. Monsoon-like climate during the Bajocian. Clay mineralogical and geochemical study on a limestone/marl alternation (Komló Calcareous Marl Formation, Mecsek Mountains, Southern Hungary). *Hantkeniana*, **3**, 149–176.

Reuning, L., Reijmer, J.J.G. & Betzler, C. 2002. Sedimentation cycles and their diagenesis on the slope of a Miocene carbonate ramp (Bahamas, ODP Leg 166). *Marine Geology*, **185**, 121–142.

Rioult, M., Contini, D., Elmi, S., Gabilly, J. & Mouterde, R. 1997. Bajocien. *In*: Cariou, E. & Hantzpergue, P. (eds) *Biostratigraphie du Jurassique ouest-européen et méditerranéen: zonations parallèles et distribution des invertébrés et microfossiles*. Bulletin des Centres de Recherches Exploration–Production Elf-Aquitaine, 41–53.

Rogov, M.A. & Zakharov, V.A. 2010. Jurassic and lower Cretaceous glendonites occurrences and their implication for Arctic paleoclimatic reconstructions and stratigraphy. *Earth Science Frontiers*, **17**, 345–347.

Sageman, B.B., Meyers, S.R. & Arthur, M.A. 2006. Orbital time scale and new C-isotope record for Cenomanian–Turonian boundary stratotype. *Geology*, **34**, 125–128.

Schlager, W., Reijmer, J.J.G. & Droxler, A. 1994. Highstand shedding of carbonate platforms. *Journal of Sedimentary Research*, **64**, 270–281.

Scotese, C.R. 2001. *Atlas of Earth History, Vol. 1*. PALEOMAP Project, Arlington, TX.

Sprovieri, M., Coccioni, R., Lirer, F., Pelosi, N. & Lozar, F. 2006. Orbital tuning of a lower Cretaceous composite record (Maiolica Formation, central Italy). *Paleoceanography*, **21**, PA4212.

Stoll, H.M. & Schrag, D.P. 2000. Coccolith Sr/Ca as a new indicator of coccolithophorid calcification and growth rate. *Geochemistry, Geophysics, Geosystems*, **1**, 1006, http://dx.doi.org/10.1029/1999GC000015

Suan, G., Mattioli, E., Pittet, B., Mailliot, S. & Lécuyer, C. 2008*a*. Evidence for major environmental perturbation prior to and during the Toarcian (Early Jurassic) oceanic anoxic event from the Lusitanian Basin, Portugal. *Paleoceanography*, **23**, PA1202.

Suan, G., Pittet, B., Bour, I., Mattioli, E., Duarte, L.V. & Mailliot, S. 2008*b*. Duration of the Early Toarcian carbon isotope excursion deduced from spectral analysis: Consequence for its possible causes. *Earth and Planetary Science Letters*, **267**, 666–679.

Suchéras-Marx, B. 2012. *Emergence de la production carbonate pélagique au Jurassique moyen (180–160 Ma)*. PhD thesis, Université Claude Bernard Lyon1, Villeurbanne.

Suchéras-Marx, B., Guihou, A., Giraud, F., Lécuyer, C., Allemand, P., Pittet, B. & Mattioli, E. 2012. Impact of the Middle Jurassic diversification of Watznaueria (coccolith-bearing algae) on the carbon cycle and $\delta^{13}C$ of bulk marine carbonates. *Global and Planetary Change*, **86–87**, 92–100.

Thiry-Bastien, P. 2002. *Stratigraphie séquentielle des calcaires bajociens de l'Est de la France (Jura–Bassin de Paris)*. PhD thesis, Université Claude Bernard Lyon1, Villeurbanne.

Torrence, C. & Compo, G.P. 1998. A practical guide to wavelet analysis. *Bulletin of the American Meteorological Society*, **79**, 61–78.

Vail, P.R., Audemard, F., Bowman, S.A., Eisner, P.N. & Perez-Cruz, C. 1991. The stratigraphic signatures of tectonics, eustasy and sedimentology—an overview. *In*: Einsele, G., Ricken, W. & Seilacher, A. (eds) *Cycles and Events in Stratigraphy*. Springer, Berlin.

Voigt, S., Gale, A.S. & Voigt, T. 2006. Sea-level change, carbon cycling and palaeoclimate during the Late Cenomanian of northwest Europe; an integrated palaeoenvironmental analysis. *Cretaceous Research*, **27**, 836–858.

Voigt, S., Erbacher, J., *et al.* 2008. The Cenomanian–Turonian of the Wunstorf section (North Germany): global stratigraphic reference section and new orbital time scale for Oceanic Anoxic Event 2. *Newsletters on Stratigraphy*, **43**, 65–89.

Weedon, G.P. 2003. *Time-Series Analysis and Cyclostratigraphy: Examining Stratigraphic Records of Environmental Cycles*. Cambridge University Press, Cambridge.

Weedon, G.P. & Jenkyns, H.C. 1999. Cyclostratigraphy and the Early Jurassic timescale; data from the Belemnite Marls, Dorset, southern England. *Geological Society of America Bulletin*, **111**, 1823–1840.

Weissert, H. & Erba, E. 2004. Volcanism, CO_2 and palaeoclimate: A Late Jurassic–Early Cretaceous carbon and oxygen isotope record. *Journal of the Geological Society, London*, **161**, 695–702.

Westphal, H., Böhm, F. & Bornholdt, S. 2004. Orbital frequencies in the carbonate sedimentary record: Distorted by diagenesis? *Facies*, **50**, 3–11.

Received 7 November 2011; revised typescript accepted 12 July 2012.
Scientific editing by James Hendry.